



Opportunistic evaluation of modelled sea ice drift using passively drifting telemetry collars in Hudson Bay, Canada

Ron R. Togunov¹, Natasha J. Klappstein², Nicholas J. Lunn³, Andrew E. Derocher², Marie Auger-Méthé⁴

¹Department of Zoology, Institute for the Oceans and Fisheries, University of British Columbia, Vancouver, BC V6T 1Z4, Canada

²Department of Biological Sciences, University of Alberta, Edmonton, AB T6G 2E9, Canada

³Wildlife Research Division, Science & Technology Branch, Environment and Climate Change Canada, CW-422 Department of Biological Sciences, University of Alberta, Edmonton, AB T6G 2E9, Canada

⁴Department of Statistics, Institute for the Oceans and Fisheries, University of British Columbia, Vancouver, BC V6T 1Z4, Canada

Correspondence to: Ron R. Togunov (r.togunov@oceans.ubc.ca)

Abstract

Sea ice drift plays a central role in the Arctic climate and ecology through its effects on the ice cover, thermodynamics, and energetics of northern marine ecosystems. Due to the challenges of accessing the Arctic, remote sensing has been used to obtain large-scale longitudinal data. These data are often associated with errors and biases that must be considered when incorporated into research. However, obtaining reference data for validation is often prohibitively expensive or practically unfeasible. We used the motion of 20 passively drifting high-accuracy GPS telemetry collars originally deployed on polar bears, *Ursus maritimus*, in western Hudson Bay, Canada to validate a widely used sea ice drift dataset produced by the National Snow and Ice Data Centre (NSIDC). Our results showed that the NSIDC model tended to underestimate the ‘horizontal’ and ‘vertical’ (i.e. ‘u’ and ‘v’) components of drift. Consequently, the NSIDC model underestimated magnitude of drift, particularly at high ice speeds. Modelled drift direction was unbiased, however it was less precise at lower drift speeds. Research using these drift data should consider integrating these biases into their analyses, particularly where absolute ground speed or direction is necessary. Further investigation is required into the sources of error, particularly in under-examined areas without in situ data.



1 Introduction

Many research fields increasingly depend on remote sensing to collect environmental data. The raw data from various remote sensing sources are often combined using modelling and interpolation techniques to create an accessible gridded product (Reichle, 2008). For example, the Hadley Centre Sea Ice and Sea Surface Temperature data set, which combines data from numerous sources including active and passive satellite sensors, ice charts, and historic records (Titchner and Rayner, 2014). However, measurement errors and assimilation biases can lead to large inaccuracies (Reichle, 2008). If the degree of measurement error is greater than the variability of the system being modelled, it could lead to spurious results (Auger-Méthé et al., 2016b). Quantifying error in remotely sensed data can be used to improve these data products (Cressie et al., 2009), and is important for data assimilation and the development of new products (Meier et al., 2000; Sumata et al., 2014, 2015a). However, assessing these errors is challenging, particularly in remote areas that are difficult to ground-truth.

Sea ice studies often rely on remotely-sensed data due to the remote, vast, and dynamic nature of the environment. Sea ice drift is a fundamental contributor to the dynamism of the Arctic ecosystem. Ice drift affects important thermodynamic processes through the formation of polynyas and leads (Marcq and Weiss, 2012), modulates ice deformation rates (Bouillon and Rampal, 2015; Rampal et al., 2009), and can determine spatial distribution and configuration of different ice ages and thicknesses (Hutchings and Rigor, 2012; Mahoney et al., 2019). It also drives the rate of sea ice export, which affects ice extent throughout the Arctic (Rampal et al., 2009). Therefore, ice drift is often considered in models of ice cover characteristics, overall sea ice mass throughout the Arctic, and global climate patterns (Hunke et al., 2010; Kimura and Wakatsuchi, 2000; Kwok et al., 2013). In addition to geographic and environmental studies, ice drift has received increased attention in ecology. Ice drift influences the distribution and biomass of plankton (Hop and Pavlova, 2008; Kohlbach et al., 2017; Onodera et al., 2015; Thorpe et al., 2007), as well as polar bear (*Ursus maritimus*) behaviour and energetics (Auger-Méthé et al., 2016a; Durner et al., 2017; Mauritzen et al., 2003). In addition to its effects on geophysics and wildlife, ice drift is also important in describing transport of microplastics in the Arctic (Peeken et al., 2018). Given its broad application, the accuracy of ice drift data is critical when drawing geophysical and ecological conclusions.

Several sources of ice drift data are available at variable spatiotemporal resolutions (Sumata et al., 2014). Although the data and models used vary between ice products, ice drift estimates are generally estimated from combinations of buoy data, weather forecast models, and satellite measurements. These data sources vary in coverage, resolution, accuracy, and sensitivity to environmental/meteorological conditions and, therefore, result in products with variable sources of error (Mahoney et al., 2019; Sumata et al., 2014). In this paper, we sought to quantify these errors in a widely employed sea ice drift data product produced by the National Snow and Ice Data Center (NSIDC; Boulder, CO): Polar Pathfinder Daily 25 km EASE-Grid Sea Ice Motion Vectors (hereafter, NSDIC drift; Tschudi et al., 2019). NSDIC drift estimates are produced by assimilating drift obtained from several satellite-based sensors, buoys, and modelled wind fields, providing among the most extensive, high resolution, and complete spatial coverage. In addition, NSDIC drift product has the longest temporal coverage of any sea ice drift products extending from 1978 to the present (Tschudi et al., 2019).



60 Although research has examined the accuracy of older versions of NSIDC drift (e.g., Ruslan I. May, 2018; Schwegmann et al., 2011; Sumata et al., 2014, 2015b), the latest major release (version 4.0) has yet to be externally evaluated. The NSIDC drift model integrates the movement of buoys from the International Arctic Buoy Program (IABP; <http://iabp.apl.washington.edu/>), and are the highest weighted input source driving the NSIDC (Sumata et al., 2015a). Regions without such in situ measurements are more susceptible to bias (Mahoney et al., 2019; Sumata et al., 2015a; Tschudi et al., 65 2019), and are therefore particularly important to evaluate.

There are three types of validation data: (1) other high resolution satellite-based estimates (e.g., Advanced Very High Resolution Radiometer (AVHRR) or Synthetic Aperture Radar (SAR), (2) moored Doppler-based velocity measures, and (3) in situ drifters, including buoys, ships, and manned stations (Lavergne, 2016). Other satellite-based estimates are associated with their own estimation errors, and Doppler-based validation represent only errors in the area in which they are moored 70 (Rozman et al., 2011). Some studies used in situ drifters (e.g., drifting research stations or buoys) as reference data, however, they are consequently limited in spatial extent (Hwang, 2013; Rozman et al., 2011; Tschudi et al., 2010). Since there are few sources of in situ sea ice drift data, some studies that quantify NSIDC drift accuracy used the same IABP data that are integrated into NSIDC model for validation, which may underestimate bias. Further, IABP buoys typically use ARGOS location estimates, which have spatial errors up to tens of kilometres and may be unsuitable for validation (Hwang, 2013).

75 In this paper, we evaluate the bias and precision (hereafter, collectively referred to as *accuracy*) of NSIDC drift data in Hudson Bay using an opportunistic and independent source of sea ice drift validation data. We compared modelled NSIDC drift to drifting GPS collars that were originally deployed on polar bears but dropped onto sea ice. There has been no study of the accuracy of any sea ice drift model in Hudson Bay. In addition, the bay does not have any IABP buoys, which drive the NSIDC model and its performance. Our objectives were to quantify drift accuracy within three domains: drift speed, drift 80 direction, and the orthogonal (horizontal, ‘u’, and vertical, ‘v’) components of the drift vectors. We also explored whether accuracy varied with the underlying drift speed, across months, or across years.

2 Methods

We fitted polar bears in western Hudson Bay, Canada with satellite-linked GPS collars (Telonics, Mesa, Arizona) in August and September of 2004-2015 (Figure 1). Procedures for animal capture and handling are described by Stirling et al. (1989) and 85 were approved annually by the University of Alberta Animal Care and Use Committee for Biosciences and by the Environment and Climate Change Canada Western and Northern Region Animal Care Committee. Protocols were in accordance with the Canadian Council on Animal Care. Collars were programmed to obtain GPS fixes every 4 h. The locations obtained are high-accuracy, with errors < 31 m (D’Eon et al., 2002). Although deployed with the purpose of studying polar bear behaviour and space use, some collars may slip off the bears, release early due to premature failure of the release mechanism, or the bear may 90 die while the collars continue to transmit locations. In these instances, the observed displacement of the collars represents the motion of sea ice. We identified drifting collars either through ‘activity’ sensors in the collars or by manually comparing the



observed collar displacement with sea ice satellite imagery (Supplement S1). To verify that manually identified drifting collars were passively drifting and not on active bears, we compared accuracy metrics for speed, direction, and u and v (relative to the NSIDC drift projection, EPSG:3408) among activity sensor collars, manually identified passive collars, and collars on active bears. Detailed methods and results of this comparison are presented in the Supplement (S2).

We used the motion of the identified drifting collars (following date of inactivity/drop off; hereafter simply, *collars*) to quantify the accuracy and precision of NSIDC drift data. The NSIDC product provides daily estimates of sea ice drift derived from buoy data, National Center for Environmental Prediction and National Center for Atmospheric Research reanalysis wind vectors, and several satellite sensors including AVHRR, The Advanced Microwave Scanning Radiometer - Earth Observing System (AMSRE), Scanning Multichannel Microwave Radiometer (SMMR), and the Special Sensor Microwave Imager / Sounder (SSMIS; Tschudi et al., 2019). To match the NSIDC product, collar locations were projected into the 25 km EASE-grid North (EPSG: 3408) projection used by NSIDC. NSIDC represents drift as movement between 12:00 UTC of subsequent days. To match the NSIDC temporal resolution, we subsampled the collar locations to a 24 h resolution by retaining locations from 13:00 UTC, the closest collar location to 12:00 UTC. Next, we calculated drift vectors/components (i.e., speed, direction, u , and v), then removed any vectors from locations > 24 h apart. Next, we interpolated the NSIDC drift to the first location of each collar drift vector using inverse distance weight (inverse distance power set to three and maximum distance of 50 km) to match the fix location.

The summary statistics chosen to quantify drift accuracy can lead to incomplete or spurious conclusions (Volkov et al., 2017). For example, root mean square and standard errors convey the magnitude of the error, but not the direction. Correlation coefficients between model and reference data describe model precision, but not accuracy. Some studies investigated the accuracy of the orthogonal components of drift (i.e., u and v) individually; however, this does not convey the accuracy in speed and direction, which are emergent properties of both components. For example, if the biases of the orthogonal components are equal and scale proportionally, then direction estimates remain accurate. Conversely, if the biases are negatively correlated, they may partially cancel and result in speed estimates more accurate than appear when examining the drift components independently. Thus, in addition to the orthogonal u and v components of drift, we also quantified the accuracy of drift speed and direction.

We tested five key questions: (1) are the estimated model speeds significantly different from the collar speeds, (2) is the relative speed accuracy dependant on the underlying drift speed being estimated, (3) are the estimated model directions significantly different from the collar directions, (4) is the direction accuracy dependant on the underlying drift speed, and (5) do the relationships between the model u (v) and collar u (v) components diverge significantly from 1. Because the data is spatiotemporally autocorrelated, with subsequent days having similar drift speeds and different collars sampling different regions of Hudson Bay, we could not use a simple paired t-test for the absolute speed bias (1). Instead, we used an intercept-only generalized linear mixed effect model (GLMM; with a Gaussian error distribution) with absolute speed bias ($Speed_{NSIDC} - Speed_{collar}$) as the response, wherein a significant intercept represents a significant difference between the model and the collar speeds. To account for repeat sampling from different collars representing different regions, collar identity



was used as a random effect. To account for temporal autocorrelation, we fit the model with a first-order autoregressive error process (AR1). For speed-dependant accuracy of model speed (2), we defined *relative speed accuracy* as the quotient of NSIDC drift speed over collar speed, $\frac{Speed_{NSIDC}}{Speed_{collar}}$, with values > 1 representing overestimation and values < 1 representing underestimation. This *relative speed accuracy* was modelled as a function of $\log(Speed_{collar})$ using GLMMs with gamma error distribution and a log-link function. We log transformed $Speed_{collar}$ because it is zero-bound and the relative difference in speed (and thus its relative effect on model accuracy) decays exponentially with increasing values. We used the same random effect and AR1 structure as in (1). We assessed the accuracy of model direction, $Direction_{NSIDC} - Direction_{collar}$, (3) using a Watson-Williams test for homogeneity of means for circular data. Although this test does not incorporate autocorrelation, the absolute direction accuracy did not exhibit temporal autocorrelation (Figure 2). For the speed-specific direction accuracy (4), we defined *relative direction accuracy* as the linearized absolute difference in direction, $\tan\left(\frac{|Direction_{NSIDC} - Direction_{collar}|}{2}\right)$, where 0 represents model unanimity and departure from 0 represents increasing error. This *relative direction accuracy* was modelled as a function of $\log(Speed_{collar})$ using the same GLMM procedures used for testing speed-specific relative speed accuracy (2). Any differences in speed or direction between the NSIDC and collar drift ultimately emerge from the estimated u and v components of sea ice drift. We assessed the relationship between the orthogonal components of NSIDC and collar drift (5) using GLMM (with a Gaussian error distribution), with model u (v) modelled as functions of collar u (v), and the same random effect and AR1 structure as in (1), (2), and (4). All GLMMs were fit using penalized quasi-likelihood (GLMM_{PQL}; Breslow and Clayton, 1993) using the ‘glmmPQL’ function of the ‘MASS’ package (Venables and Ripley, 2002). Using GLMM_{PQL}, enabled us to meet all our model criteria: non-linear models with random effects and an auto-regressive structure. As a broad metric of goodness of fit, we used a the GLMM_{PQL} R^2 metric developed by Jaeger et al. (2017) using the ‘r2beta’ function in ‘r2glmm’ package. All data processing and analyses were conducted in R version 3.6.1 (R Core Team, 2019).

3 Results

We identified 20 drifting collars with locations from December-July of 2005-2015 (Figure 1 and Figure 3), with a mean of 520 ± 358 GPS fixes per collar (total = 10409). The largest number of identified collars in one year was in 2009 (n = 6). The motion for these six collars is depicted in the supplement video (<http://doi.org/10.5446/45186>), which depicts the large degree of concurrence of drift vectors across large spatial extent. After subsampling to a daily resolution, we analysed 1677 collar drift vectors. The number of drift vectors ranged from 71 vectors in July to 304 vectors in March (mean = 210 ± 83 vectors; Figure 4).



3.1 Accuracy of NSIDC drift speed

155 Mean NSIDC drift speed was 5.8 ± 4.5 km d⁻¹ while mean collar speed was 8.4 ± 7.1 km d⁻¹, the difference in speed $Speed_{NSIDC} - Speed_{collar}$ was statistically significant (GLMM_{PQL}: intercept \pm 95 % CI = -3.0 ± 1.2 km d⁻¹, df = 1657, t = -4.8, p < 0.0001; Figure 5). NSIDC drift speeds were slower than collar drift speeds in 63.1% of the vectors and only 10.4 % of NSIDC drift speeds were within \pm 10 % of collar drift speeds (Figure 5a). The discrepancy in drift speed was more pronounced at higher collar drift speeds, with a significant relationship between the quotient ($\frac{Speed_{NSIDC}}{Speed_{collar}}$) and collar speed
160 (GLMM_{PQL}: slope = -0.67, df = 1656, t_{slope} = -38.80, p_{slope} < 0.0001, R² = 0.53; Figure 5b). Collar drift speeds < 4.5 km d⁻¹ were overestimated by a median of 42 %, speeds between 4.5 and 9.0 km d⁻¹ were underestimated by a median of 26 %, and speeds > 9.0 km d⁻¹ were underestimated by a median of 51 % (Figure 5). There was intra-annual and inter-annual variation (based on 95% CIs) in the correlation of NSIDC drift speeds and collar drift speeds, however there was no apparent pattern (Figure 3 and Figure 4).

165 3.2 Accuracy of NSIDC drift direction

NSIDC drift directions were on average $2.6^\circ \pm 53.9^\circ$ left relative to the collar drift direction, although the mean difference was not significantly different from 0° (Watson-Williams test: df₁ = 1, df₂ = 1676, F = 0.003, p = 0.95; Figure 6 and Figure 7). Most (71.3 %) of the NSIDC drift directions were within \pm 22.5° of the collar drift directions (Figure 7). NSIDC drift direction tended to be more accurate at higher collar drift speeds, with a significant relationship between relative direction accuracy and
170 collar drift speeds (GLMM_{PQL}: slope = -0.83, df = 1656, t_{slope} = -7.52, p_{slope} < 0.0001, R² = 0.03; Figure 7).

3.3 Accuracy of orthogonal NSIDC drift components

Mean collar drift u component was -0.9 ± 7.7 km d⁻¹ compared to -0.7 ± 4.3 km d⁻¹ for NSIDC drift u drift. Mean collar drift v component was -1.1 ± 7.7 km d⁻¹ compared to -0.8 ± 4.5 km d⁻¹ for NSIDC drift v component drift. NSIDC and collar drift
175 components were significantly related in both the u component (GLMM_{PQL}: slope \pm 95 % CI = 0.38 ± 0.02 , df = 1656, t_{slope} = 37.58, p_{slope} < 0.0001, R² = 0.46; Figure 8), and v component (GLMM_{PQL}: slope \pm 95 % CI = 0.40 ± 0.02 , df = 1656, t_{slope} = 37.54, p_{slope} < 0.0001, R² = 0.52; Figure 8). Although the components of NSIDC drift and collar drift were significantly correlated, the slopes of the regression were significantly underestimated (indicated by the slope estimate and 95 % CI being < 1).

180 4 Discussion

Using drifting collars as reference data for validation, we identified biases in the NSIDC modelled sea ice drift. NSIDC drift speeds tended to be underestimated, although drift direction was relatively accurate. This is due to the underestimation of u



and v components, which showed a similar magnitude in their bias. The biases in speed and direction were related to the underlying drift speed as measured by the collars. NSIDC drift speeds tended to overestimate slow collar drift ($< 4.5 \text{ km h}^{-1}$) and underestimate high collar drift ($> 4.5 \text{ km h}^{-1}$). This pattern is likely an effect of estimating a zero-bound variable, and is consistent with other satellite-based sea ice drift products (Johansson and Berg, 2016; Mahoney et al., 2019; Rozman et al., 2011; Sumata et al., 2014). As drift speeds approach 0 km d^{-1} , the probability of overestimation approaches 1, and as drift speeds increase, the range of values that below the drift speed (i.e., underestimates) increases. Although the bias is mathematically inevitable to some degree, the magnitude of the bias is not fixed and our results show that the error can be high, with drift speeds underestimated by a median of 22.9% (1.4 km d^{-1}). This is similar to the drift bias observed by Durner et al., (2017) in the Beaufort and Chukchi Seas, wherein mean daily model speed was underestimated by a mean of 28.0% (2.25 km d^{-1}). These biases are small relative to the 25 km resolution of the satellite input data, however in some analyses, the bias would compound over time. For example, cumulative/total daily drift calculated for 7 months (corresponding to the months in which we obtained drift data) would be underestimated by $> 295 \text{ km}$. Drift direction accuracy increased at higher collar drift speeds. This is probably because magnitude and uniformity of sea ice displacement increase with drift speed, and more likely to be detected by NSIDC's feature-matching algorithm (based on maximum cross-correlation; Tschudi et al., 2019).

Our estimates of drift speed bias are greater than estimated in studies of NSIDC and other drift products (Hwang, 2013; Johansson and Berg, 2016; Lavergne, 2016; Schwegmann et al., 2011; Sumata et al., 2014; but see Durner et al., 2017). However, the Hudson Bay system is different from areas where drift accuracy has been studied. Hudson Bay has a smaller area to shoreline ratio due to its smaller size compared to the rest of the Arctic Ocean (excluding the Canadian Archipelago), which confounds satellite and wind-based drift estimation (Thorndike and Colony, 1982; Tschudi et al., 2019). Satellite-based tracking relies on a feature-matching algorithm, and cannot resolve velocities near the shore (Heil et al., 2001; Meier et al., 2000; Tschudi et al., 2019). Wind-based drift estimates assume a 1 % relationship with speed and 45° relationship with direction, however near the coast, internal ice stress/forces can match and exceed those of wind and currents (Thorndike and Colony, 1982). Thorndike and Colony (1982) estimated the effects of the coast on drift to extend up to 400 km , which is the approximate radius of Hudson Bay. The bay is a seasonal system, completely melting in summer and reaching nearly 100 % cover in winter (Danielson, 1971; Saucier et al., 2004; Stewart and Barber, 2010). Consequently, sea ice in Hudson Bay lacks multi-year ice, and the ice is younger and generally thinner, with extensive periods of low concentration, factors which both decrease accuracy of modelled ice drift (Durner et al., 2017; Mahoney et al., 2019; Sumata et al., 2014). At low ice concentrations, satellites sensors are more likely not to detect sea ice (Castro De La Guardia et al., 2017; Tivy et al., 2011). The formation of new sea ice during freeze-up and the melt pools that form during break-up both confound estimation of drift (Meier et al., 2000; Tschudi et al., 2019; Willmes et al., 2009). Lastly, there are no IABP buoys in Hudson Bay to contribute data to the NSIDC drift model, another factor associated with poorer model performance (Mahoney et al., 2019; Tschudi et al., 2019). Earlier versions of NSIDC drift products (see Tschudi et al., 2016) effectively limited the influence of buoys to $\sim 350 \text{ km}$, which introduced artefacts around buoy locations (Szanyi et al., 2016). Changes to the algorithm in version 4 of



NSIDC drift eliminated the artefacts and increased accuracy within the Arctic Ocean (Tschudi et al., 2019), however, these changes would not have improved drift estimates in regions without buoy data, including Hudson Bay.

220 The drift biases we report are limited by availability of telemetry collar data, and we cannot definitively extrapolate
our accuracy estimates beyond this spatiotemporal extent. A common limitation of these types of studies is the reliance on
interpolation. Bilinear, or inverse distance weighted, interpolation yields estimates that tend towards the mean and precludes
obtaining outermost estimates (Schwegmann et al., 2011). In addition, interpolation within skewed distributions is likely to
yield spurious estimates. For example, in right-skewed datasets (e.g., zero-bound drift speed), outliers are more likely greater
than the mean and inverse-distance averaging is more likely to be an overestimate. Nevertheless, there is no reason to believe
225 these biases would be greater than those of other sea ice drift validation studies that used linear interpolation to match satellite
with in situ based estimates (Lavergne, 2016; Schwegmann et al., 2011).

The EASE-Grid projection is polar azimuthal and induces meridional compression and zonal stretching, which further
biases drift estimation. The effect of this distortion is that north-south (east-west) drift is more likely to be underestimated
(overestimated) and direction estimates will be biased toward the east-west axis. This bias is amplified as you approach the
230 equatorial limits of dataset and is particularly important if ground-speed is required. Many of the biases we present have been
reported in research of NSIDC and other satellite-based sea ice drift estimates (Heil et al., 2001; Karlsson, 2016; Lavergne,
2016; Linow et al., 2015; Rozman et al., 2011; Schwegmann et al., 2011; Sumata et al., 2014, 2015b, 2015a; Szanyi et al.,
2016). Assuming the overall NSIDC drift accuracy is consistent over time, these data are likely well-suited for addressing
questions where the *relative* speed or direction are sufficient, for example longitudinal analyses such as climate-induced
235 changes in drift speed (e.g., Kwok et al., 2013; Klappstein et al. in review). Still, large error may obscure underlying trends.
We suggest cautious application of the NSIDC drift data where the *absolute* speed or direction is critical. For example,
calculation of animal energetics (e.g., Durner et al., 2017; Klappstein et al., in review), home ranges (e.g., Auger-Méthé et al.,
2016a), voluntary movement (e.g., Togunov et al., 2017, 2018), and predicting/retrodicting distribution of drifting matter
(Kohlbach et al., 2017; Peeken et al., 2018; Thorpe et al., 2007; Tschudi et al., 2010). The degree of error/bias that is
240 permissible is research-specific. Generally, to be able to correctly account for measurement error, it has to be smaller than the
natural stochasticity of the system being studied (Auger-Méthé et al., 2016b). Particular attention to error/bias should be given
in regions without IABP buoy data or where bias is unquantified.

5 Conclusions

This study provides the first error estimates of any sea ice drift model in Hudson Bay. Using passively drifting telemetry
245 collars, we quantified the accuracy and precision of Polar Pathfinder Daily 25 km EASE-Grid Sea Ice Motion Vectors (Version
4). Both *u* and *v* components of NSIDC drift along with the resultant speed tended to systematically underestimate true drift
speed, a pattern exacerbated at higher speeds. The direction showed no systematic bias, however directional precision



decreased at lower speeds. We suggest that any research requiring absolute values for drift speed/direction should account for error/bias of drift in the study design and/or test the sensitivity of the results to these biases (Cressie et al., 2009).

250 Although our collar GPS data were collected with the intent of studying polar bear ecology, we believe it and other forms of animal-borne telemetry can be of great utility in advancing environmental modelling. For example, polar bear telemetry has been used to validate sea ice drift in the Beaufort and Chukchi Seas (Durner et al., 2017; Tschudi et al., 2010) and assess accuracy of sea ice concentration data (Castro De La Guardia et al., 2017), and seabird tracking has been used to estimate ocean currents and wind velocities (Goto et al., 2017; Yoda et al., 2014; Yonehara et al., 2016). In addition to being
255 useful for model validation, these types of data can be incorporated into environmental models as additional data streams, providing insight into areas that are more difficult to measure (Harcourt et al., 2019; Miyazawa et al., 2015). To help improve modelled drift data, we have made the position data of our drifting collars public ([This data will be made available on the Dataverse Project]). The data can also be used to identify error/bias associated with different locations, periods, or environmental conditions (e.g., ice thickness, ice concentration, and cloud cover) in which models can be improved (e.g.,
260 Miyazawa et al., 2015). Our study provides evidence of modelled ice drift bias in Hudson Bay, where lack of Arctic buoys makes this type of study difficult. Ultimately, these findings (in combination with our public data set) can be a good resource for quantifying and validating the accuracy of other and/or future ice drift products.

Data availability

The Polar Pathfinder Daily 25 km EASE-Grid Sea Ice Motion Vectors (Version 4) dataset is available at
265 (<https://nsidc.org/data/nsidc-0116/versions/4>, last access: 22 December 2019). The location data of the passively drifting collars is available at ([URL], last access: [])

Author contributions

RT identified the drifting collars. RT and NK designed the study and conducted the analyses with contributions from MAM and AD. NL and AD conducted field work with assistance from RT and NK. RT prepared the manuscript with contributions
270 from all authors.

Competing interests

The authors declare that they have no conflict of interest.



Acknowledgments

Financial and logistical support of this study was provided by Canadian Association of Zoos and Aquariums, the Canadian
275 Research Chairs program, the Churchill Northern Studies Centre, Canadian Wildlife Federation, Care for the Wild
International, Earth Rangers Foundation, Environment and Climate Change Canada, Hauser Bears, the Isdell Family
Foundation, Kansas City Zoo, Manitoba Sustainable Development, Natural Sciences and Engineering Research Council of
Canada, Parks Canada Agency, Pittsburgh Zoo Conservation Fund, Polar Bears International, Quark Expeditions, Schad
Foundation, Sigmund Soudack & Associates Inc., Wildlife Media Inc., and World Wildlife Fund Canada.

280 References

- Auger-Méthé, M., Lewis, M. A. and Derocher, A. E.: Home ranges in moving habitats: Polar bears and sea ice, *Ecography*
(Cop.), 39(1), 26–35, doi:10.1111/ecog.01260, 2016a.
- Auger-Méthé, M., Field, C., Albertsen, C. M., Derocher, A. E., Lewis, M. A., Jonsen, I. D. and Flemming, J. M.: State-space
models' dirty little secrets: Even simple linear Gaussian models can have estimation problems, *Sci. Rep.*, 6, 26677,
285 doi:10.1038/srep26677, 2016b.
- Bouillon, S. and Rampal, P.: On producing sea ice deformation data sets from SAR-derived sea ice motion, *Cryosph.*, 9, 663–
673, doi:10.5194/tc-9-663-2015, 2015.
- Breslow, N. E. and Clayton, D. G.: Approximate inference in generalized linear mixed models, *J. Am. Stat. Assoc.*, 88(421),
9, doi:10.2307/2290687, 1993.
- 290 Castro De La Guardia, L., Myers, P. G., Derocher, A. E., Lunn, N. J. and Terwisscha Van Scheltinga, A. D.: Sea ice cycle in
western Hudson Bay, Canada, from a polar bear perspective, *Mar. Ecol. Prog. Ser.*, 564, 225–233, doi:10.3354/meps11964,
2017.
- Cressie, N., Calder, C. A., Clark, J. S., Hoef, J. M. Ver and Wikle, C. K.: Accounting for uncertainty in ecological analysis:
the strengths and limitations of hierarchical statistical modeling NOEL, *Ecol. Appl.*, 19(3), 553–570, 2009.
- 295 D'Eon, R. G., Serrouya, R., Smith, G. and Kochanny, C. O.: GPS radiotelemetry error and bias in mountainous terrain, *Wildl.*
Soc. Bull., 30(2), 430–439, 2002.
- Danielson, E. W.: Hudson Bay ice conditions, *Arctic*, 24(2), 90–107, 1971.
- Durner, G. M., Douglas, D. C., Albekeke, S. E., Whiteman, J. P., Amstrup, S. C., Richardson, E. S., Wilson, R. R. and Merav,
B.-D.: Increased Arctic sea ice drift alters adult female polar bear movements and energetics, *Glob. Chang. Biol.*, 23(9), 3460–
300 3473, 2017.
- Goto, Y., Yoda, K. and Sato, K.: Asymmetry hidden in birds' tracks reveals wind, heading, and orientation ability over the
ocean, *Sci. Adv.*, 3(9), e1700097, doi:10.1126/sciadv.1700097, 2017.
- Harcourt, R., Sequeira, A. M. M., Zhang, X., Roquet, F., Komatsu, K., Heupel, M., McMahon, C., Whoriskey, F., Meekan,
M., Carroll, G., Brodie, S., Simpfendorfer, C., Hindell, M., Jonsen, I., Costa, D. P., Block, B., Muelbert, M., Woodward, B.,



- 305 Weise, M., Aarestrup, K., Biuw, M., Boehme, L., Bograd, S. J., Cazau, D., Charrassin, J.-B., Cooke, S. J., Cowley, P., de Bruyn, P. J. N., Jeanniard du Dot, T., Duarte, C., Eguíluz, V. M., Ferreira, L. C., Fernández-Gracia, J., Goetz, K., Goto, Y., Guinet, C., Hammill, M., Hays, G. C., Hazen, E. L., Hückstädt, L. A., Huveneers, C., Iverson, S., Jaaman, S. A., Kittiwattanawong, K., Kovacs, K. M., Lydersen, C., Moltmann, T., Naruoka, M., Phillips, L., Picard, B., Queiroz, N., Reverdin, G., Sato, K., Sims, D. W., Thorstad, E. B., Thums, M., Treasure, A. M., Trites, A. W., Williams, G. D., Yonehara, Y. and Fedak, M. A.: Animal-Borne Telemetry: An Integral Component of the Ocean Observing Toolkit, *Front. Mar. Sci.*, 6(6), 326, doi:10.3389/fmars.2019.00326, 2019.
- Heil, P., Fowler, C. W., Maslanik, J. A., Emery, W. J. and Allison, I.: A comparison of East Antarctic sea-ice motion derived using drifting buoys and remote sensing, *Ann. Glaciol.*, 52(57), 103–110, 2001.
- Hop, H. and Pavlova, O.: Distribution and biomass transport of ice amphipods in drifting sea ice around Svalbard, *Deep. Res. Part II*, 55(20–21), 2292–2307, doi:10.1016/j.dsr2.2008.05.023, 2008.
- 315 Hunke, E. C., Lipscomb, W. H. and Turner, A. K.: Sea-ice models for climate study: retrospective and new directions, *J. Glaciol.*, 56(200), 1162–1172, 2010.
- Hutchings, J. K. and Rigor, I. G.: Role of ice dynamics in anomalous ice conditions in the Beaufort Sea during, *J. Geophys. Res.*, 117, C00E04, doi:10.1029/2011JC007182, 2012.
- 320 Hwang, B.: Inter-comparison of satellite sea ice motion with drifting buoy data, *Int. J. Remote Sens.*, 34(24), 8741–8763, doi:10.1080/01431161.2013.848309, 2013.
- Jaeger, B. C., Edwards, L. J., Das, K. and Sen, P. K.: An R² statistic for fixed effects in the generalized linear mixed model, *J. Appl. Stat.*, 44(6), 1086–1105, doi:10.1080/02664763.2016.1193725, 2017.
- Johansson, A. M. and Berg, A.: Agreement and Complementarity of Sea Ice Drift Products, *IEEE J. Sel. Top. Appl. Earth Obs. Remote Sens.*, 9(1), 369–380, doi:10.1109/JSTARS.2015.2506786, 2016.
- 325 Karlsson, S.: Arctic sea ice drift: A comparison of modeled and remote sensing data, Lund University., 2016.
- Kimura, N. and Wakatsuchi, M.: Relationship between sea-ice motion and geostrophic wind in the Northern Hemisphere, *Geophys. Res. Lett.*, 27(22), 3735–3738, doi:10.1029/2000GL011495, 2000.
- Klappstein, N. J., Togunov, R. R., Lunn, N. J., Reimer, J. R. and Derocher, A. E.: Patterns of ice drift and polar bear (*Ursus maritimus*) movement in Hudson Bay, *Rev.*, n.d.
- 330 Kohlbach, D., Lange, B. A., Schaafsma, F. L., David, C., Vortkamp, M., Graeve, M., van Franeker, J. A., Krumpfen, T. and Flores, H.: Ice algae-produced carbon is critical for overwintering of antarctic krill *Euphausia superba*, *Front. Mar. Sci.*, 4(9), 310, doi:10.3389/fmars.2017.00310, 2017.
- Kwok, R., Spreen, G. and Pang, S.: Arctic sea ice circulation and drift speed: Decadal trends and ocean currents, *J. Geophys. Res. Ocean.*, 118(5), 2408–2425, doi:10.1002/jgrc.20191, 2013.
- 335 Lavergne, T.: Validation and Monitoring of the OSI SAF Low Resolution Sea Ice Drift Product. [online] Available from: http://osisaf.met.no/docs/osisaf_cdop2_ss2_valrep_sea-ice-drift-lr_v5p0.pdf, 2016.
- Linow, S., Hollands, T. and Dierking, W.: An assessment of the reliability of sea-ice motion and deformation retrieval using



- SAR images, *Ann. Glaciol.*, 56(69), 229–234, doi:10.3189/2015AoG69A826, 2015.
- 340 Mahoney, A. R., Hutchings, J. K., Eicken, H. and Haas, C.: Changes in the thickness and circulation of multiyear ice in the Beaufort gyre determined from pseudo-Lagrangian methods from 2003–2015, *J. Geophys. Res. Ocean.*, 124(8), 5618–5633, doi:10.1029/2018jc014911, 2019.
- Marcq, S. and Weiss, J.: Influence of sea ice lead-width distribution on turbulent heat transfer between the ocean and the atmosphere, *Cryosphere*, 6(1), 143–156, doi:10.5194/tc-6-143-2012, 2012.
- 345 Mauritzen, M., Derocher, A. E., Pavlova, O. and Wiig, Ø.: Female polar bears, *Ursus maritimus*, on the Barents Sea drift ice: walking the treadmill, *Anim. Behav.*, 66(1), 107–113, doi:10.1006/anbe.2003.2171, 2003.
- Meier, W. N., Maslanik, J. A. and Fowler, C. W.: Error analysis and assimilation of remotely sensed ice motion within an Arctic sea ice model, *J. Geophys. Res. Ocean.*, 105(C2), 3339–3356, doi:10.1029/1999jc900268, 2000.
- Miyazawa, Y., Guo, X., Varlamov, S. M., Miyama, T., Yoda, K., Sato, K., Kano, T. and Sato, K.: Assimilation of the seabird
350 and ship drift data in the north-eastern sea of Japan into an operational ocean nowcast/forecast system, *Sci. Rep.*, 5, 17672, doi:10.1038/srep17672, 2015.
- Onodera, J., Watanabe, E., Harada, N. and Honda, M. C.: Diatom flux reflects water-mass conditions on the southern Northwind Abyssal Plain, Arctic Ocean, *Biogeosciences*, 12(5), 1373–1385, doi:10.5194/bg-12-1373-2015, 2015.
- Peeken, I., Primpke, S., Beyer, B., Gütermann, J., Katlein, C., Krumpfen, T., Bergmann, M., Hehemann, L. and Gerds, G.:
355 Arctic sea ice is an important temporal sink and means of transport for microplastic, *Nat. Commun.*, 9(1), 1505, doi:10.1038/s41467-018-03825-5, 2018.
- R Core Team: R: A language and environment for statistical computing, [online] Available from: <https://www.r-project.org/>, 2019.
- Rampal, P., Weiss, J. and Marsan, D.: Positive trend in the mean speed and deformation rate of Arctic sea ice, 1979–2007, *J.*
360 *Geophys. Res. Ocean.*, 114(5), C005066, doi:10.1029/2008JC005066, 2009.
- Reichle, R. H.: Data assimilation methods in the Earth sciences, *Adv. Water Resour.*, 31(11), 1411–1418, doi:10.1016/j.advwatres.2008.01.001, 2008.
- Rozman, P., Hölemann, J. A., Krumpfen, T., Gerdes, R., Köberle, C., Lavergne, T., Adams, S. and Girard-Ardhuin, F.:
Validating satellite derived and modelled sea-ice drift in the Laptev Sea with in situ measurements from the winter of 2007/08,
365 *Polar Res.*, 30(1), 7218, doi:10.3402/polar.v30i0.7218, 2011.
- Ruslan I. May: Verification of sea ice drift data obtained from remote sensing information, in IGARSS, pp. 7344–7347, IEEE, Valencia, Spain., 2018.
- Sandvik, B.: World Borders Dataset, Themat. Mapp. [online] Available from: http://thematicmapping.org/downloads/world_borders.php (Accessed 21 January 2020), 2009.
- 370 Saucier, F. J., Senneville, S., Prinsenber, S., Roy, F., Smith, G., Gachon, P., Caya, D. and Laprise, R.: Modelling the sea ice-ocean seasonal cycle in Hudson Bay, Foxe Basin and Hudson Strait, Canada, *Clim. Dyn.*, 23(3–4), 303–326, doi:10.1007/s00382-004-0445-6, 2004.



- Schwegmann, S., Haas, C., Fowler, C. W., Gerdes, R., Heil, P., Fowler, C. W., Maslanik, J. A., Emery, W. J. and Allison, I.: A comparison of satellite-derived sea-ice motion with drifting-buoy data in the Weddell Sea, Antarctica, *Ann. Glaciol.*, 52(57), 103–110, doi:10.3189/172756411795931813, 2011.
- Stewart, D. B. and Barber, D. G.: The ocean-sea ice-atmosphere system of the Hudson Bay Complex, in *A Little Less Arctic: Top Predators in the World's Largest Northern Inland Sea, Hudson Bay*, edited by S. H. Ferguson, L. L. Loseto, and M. L. Mallory, pp. 1–37, Springer, New York, NY, USA., 2010.
- Stirling, I., Spencer, C. and Andriashek, D. S.: Immobilization of polar bears (*Ursus maritimus*) with Telazol® in the Canadian Arctic, *J. Wildl. Dis.*, 25(2), 159–168, doi:10.7589/0090-3558-25.2.159, 1989.
- Sumata, H., Lavergne, T., Girard-Ardhuin, F., Kimura, N., Tschudi, M. A., Kauker, F., Karcher, M. and Gerde, R.: An intercomparison of Arctic ice drift products to deduce uncertainty estimates, *J. Geophys. Res. Ocean.*, 119(8), 2121–2128, doi:10.1002/jgrc.20224, 2014.
- Sumata, H., Gerdes, R., Kauker, F. and Karcher, M.: Empirical error functions for monthly mean Arctic sea-ice drift, *J. Geophys. Res. Ocean.*, 120(11), 7450–7475, doi:10.1002/jgrc.20224, 2015a.
- Sumata, H., Kwok, R., Udiger Gerdes, R., Kauker, F., Karcher, M., Gerdes, R., Kauker, F. and Karcher, M.: Uncertainty of Arctic summer ice drift assessed by high-resolution SAR data, *J. Geophys. Res. Ocean.*, 120(8), 2121–2128, doi:10.1002/jgrc.20224, 2015b.
- Szanyi, S., Lukovich, J. V, Barber, D. G. and Haller, G.: Persistent artifacts in the NSIDC ice motion data set, *Geophys. Res. Lett.*, 43(20), 10800–10807, doi:10.1002/2016GL069799. Received, 2016.
- Thorndike, A. S. and Colony, R.: Sea ice motion in response to geostrophic winds, *J. Geophys. Res.*, 87(C8), 5845, doi:10.1029/jc087ic08p05845, 1982.
- Thorpe, S. E., Murphy, E. J. and Watkins, J. L.: Circumpolar connections between Antarctic krill (*Euphausia superba Dana*) populations: Investigating the roles of ocean and sea ice transport, *Deep. Res. Part I Oceanogr. Res. Pap.*, 54(5), 792–810, doi:10.1016/j.dsr.2007.01.008, 2007.
- Titchner, H. A. and Rayner, N. A.: The Met Office Hadley Centre sea ice and sea surface temperature data set, version 2: 1. Sea ice concentrations, *J. Geophys. Res. Atmos.*, 119(10), 2864–2889, doi:10.1002/2014JD021606, 2014.
- Tivy, A., Howell, S. E. L., Alt, B., McCourt, S., Chagnon, R., Crocker, G., Carrieres, T. and Yackel, J. J.: Trends and variability in summer sea ice cover in the Canadian Arctic based on the Canadian Ice Service Digital Archive, 1960–2008 and 1968–2008, *J. Geophys. Res. Ocean.*, 116(C3), C03007, doi:10.1029/2009JC005855, 2011.
- Togunov, R. R., Derocher, A. E. and Lunn, N. J. N. J.: Windscapes and olfactory foraging in a large carnivore, *Sci. Rep.*, 7, 46332, doi:10.1038/srep46332, 2017.
- Togunov, R. R., Derocher, A. E. and Lunn, N. J.: Corrigendum: Windscapes and olfactory foraging in a large carnivore (Scientific Reports DOI: 10.1038/srep46332), *Sci. Rep.*, 8, 46968, doi:10.1038/srep46968, 2018.
- Tschudi, M., Fowler, C. W., Maslanik, J. A. and Stroeve, J.: Tracking the movement and changing surface characteristics of Arctic sea ice, *IEEE J. Sel. Top. Appl. Earth Obs. Remote Sens.*, 3(4), 536–540, doi:10.1109/JSTARS.2010.2048305, 2010.



- 410 Tschudi, M. A., Fowler, C. W., Maslanik, J. A., Stewart, J. S. and Meier, W.: Polar Pathfinder daily 25 km EASE-Grid Sea Ice motion vectors, version 3. National Snow and Ice Data Center Distributed Active Archive Center., NASA Natl. Snow Ice Data Cent. Distrib. Act. Arch. Cent. [online] Available from: <https://nsidc.org/data/nsidc-0116/versions/3> (Accessed 19 October 2019), 2016.
- Tschudi, M. A., Meier, W. N. and Stewart, J. S.: An enhancement to sea ice motion and age products, *Cryosph. Discuss.*, doi:10.5194/tc-2019-40, 2019.
- Venables, W. N. and Ripley, B. D.: *Modern Applied Statistics with S*, 4th ed., Springer-Verlag, New York., 2002.
- 415 Volkov, V. A., Demchev, D. M. and Ivanov, N. E.: Validation of the model obtained ice drift fields based on satellite derived data using a vector correlation indexes in an invariant form, *J. Shipp. Ocean Eng.*, 7(6), 250–261, doi:10.17265/2159-5879/2017.06.003, 2017.
- Willmes, S., Haas, C., Nicolaus, M. and Bareiss, J.: Satellite microwave observations of the interannual variability of snowmelt on sea ice in the Southern Ocean, *J. Geophys. Res. Ocean.*, 114(3), C03006, doi:10.1029/2008JC004919, 2009.
- 420 Yoda, K., Shiomi, K. and Sato, K.: Foraging spots of streaked shearwaters in relation to ocean surface currents as identified using their drift movements, *Prog. Oceanogr.*, 122, 54–64, doi:10.1016/j.pocean.2013.12.002, 2014.
- Yonehara, Y., Goto, Y., Yoda, K., Watanuki, Y., Young, L. C., Weimerskirch, H., Bost, C. A. and Sato, K.: Flight paths of seabirds soaring over the ocean surface enable measurement of fine-scale wind speed and direction, *Proc. Natl. Acad. Sci.*, 113(32), 9039–9044, doi:10.1073/pnas.1523853113, 2016.



425

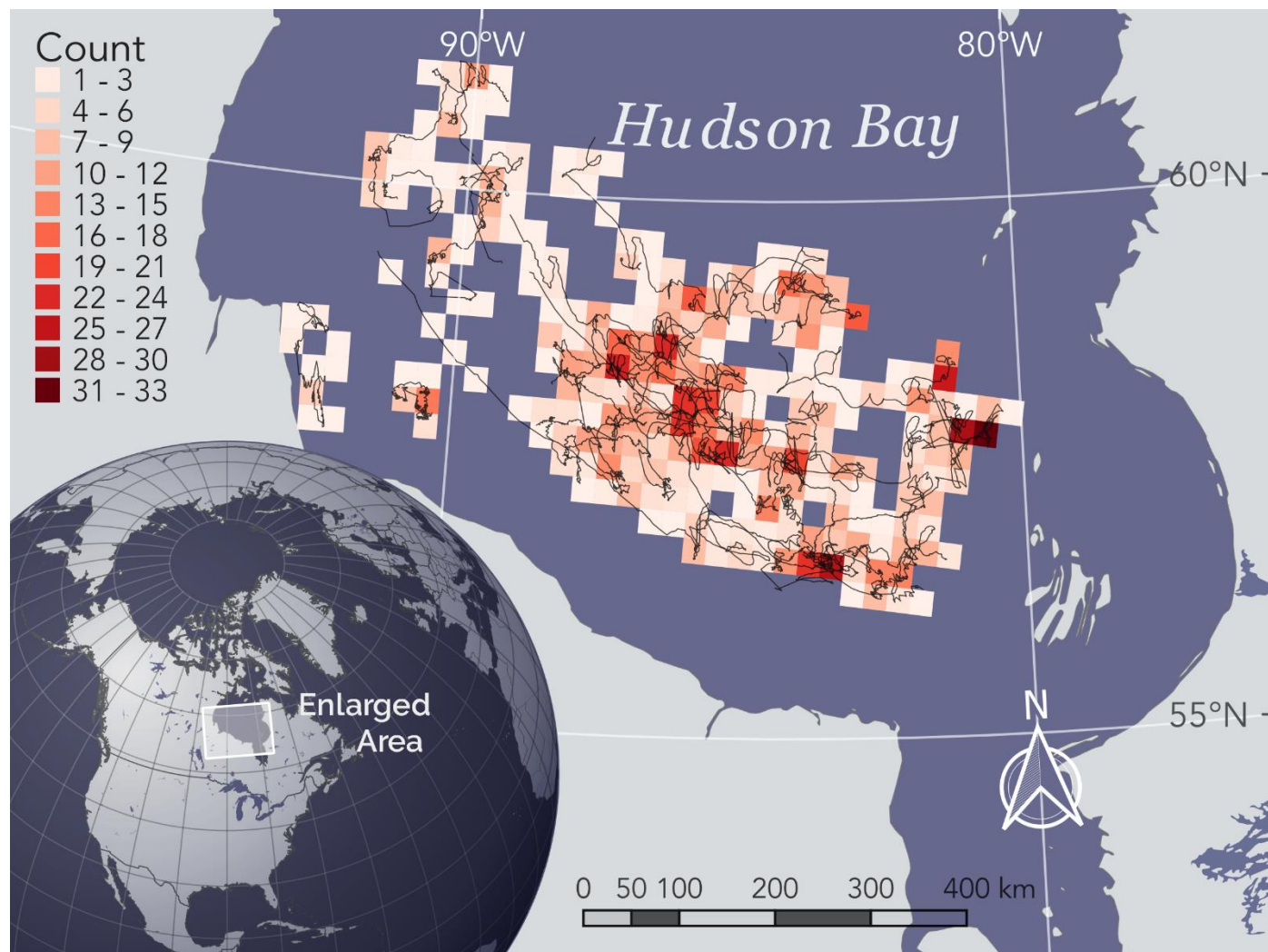
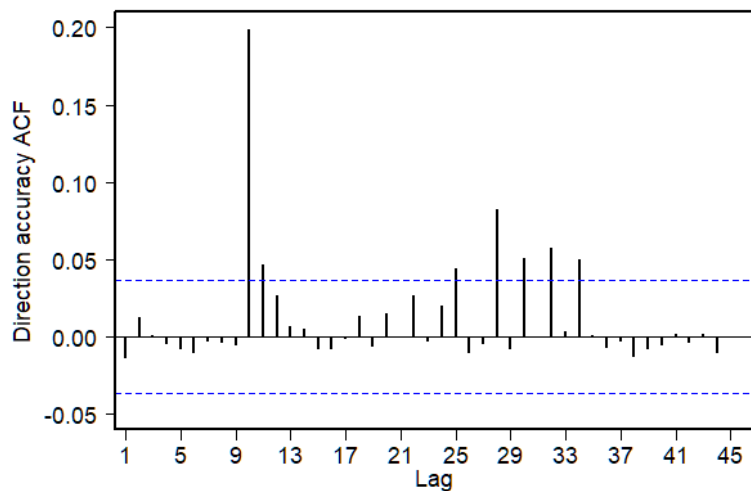
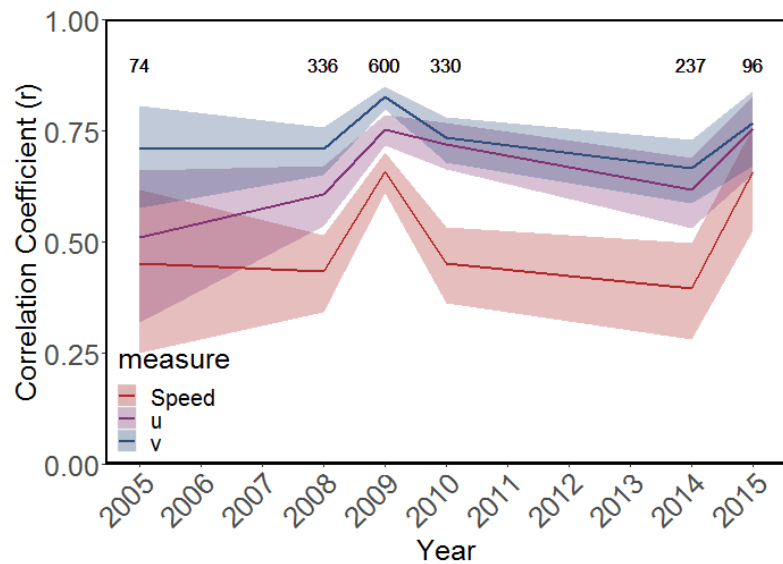


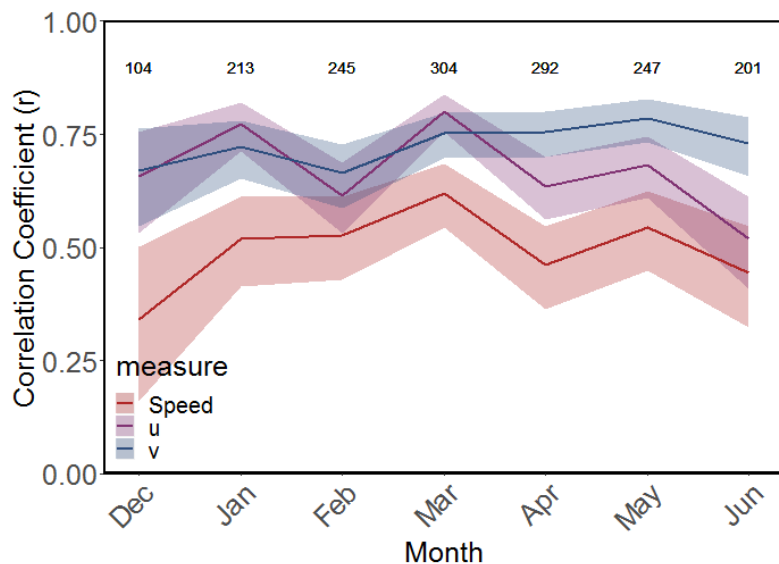
Figure 1. Hudson Bay study area (enlarged), tracks of dropped collars (black lines), and count of drift vectors (shaded cells, projected in 25 km EASE-grid North, EPSG: 3408). World borders dataset obtained from Sandvik (2009).



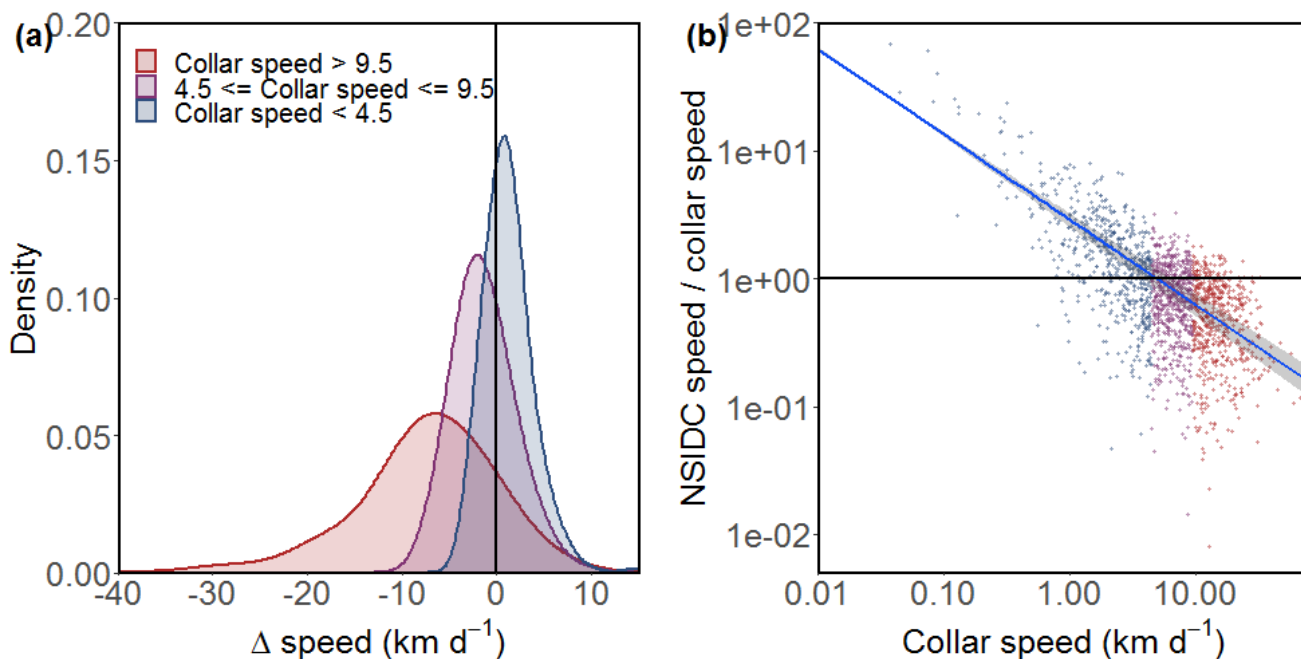
430 **Figure 2. Auto-correlation function (ACF) for NSIDC linearized direction accuracy, $\tan(|Direction_{NSIDC} - Direction_{collar}|/2)$. Blue lines correspond to the 95% CI limits that represent significant autocorrelation.**



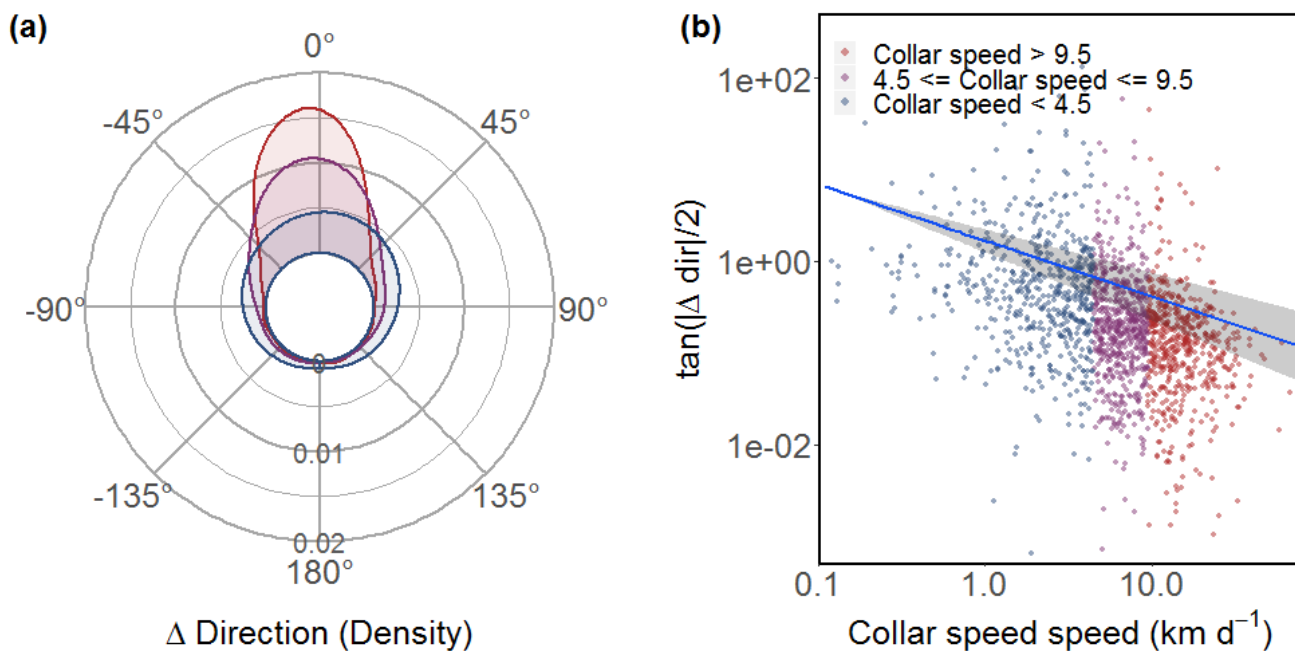
435 **Figure 3. Interannual variation in correlation coefficients (r) between NSIDC drift and collar drift speed (red line), u component (purple line), and v component (blue line). Shaded areas represent the 95% CI of the correlation coefficient. Numbers at the top represent the number of drift vectors compared in each year. 2013 excluded due to insufficient data n = 4.**



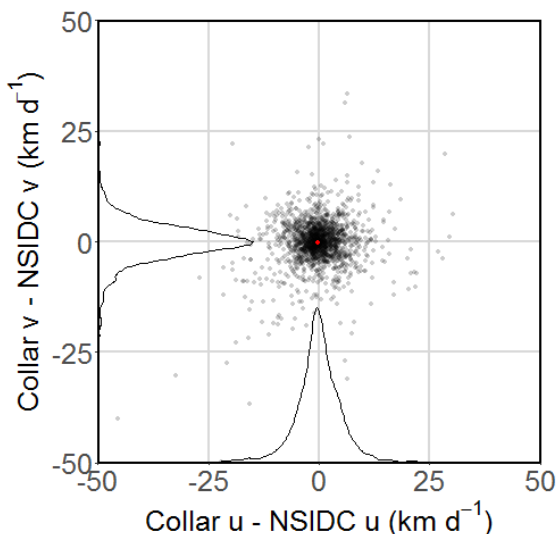
440 **Figure 4.** Intra-annual variation in correlation coefficients (r) between NSIDC drift and collar drift speed (red line), u component (purple line), and v component (blue line). Shaded areas represent the 95% CI of the correlation coefficient. Numbers at the top represent the number of drift vectors compared in each month. July excluded due to insufficient data $n = 71$.



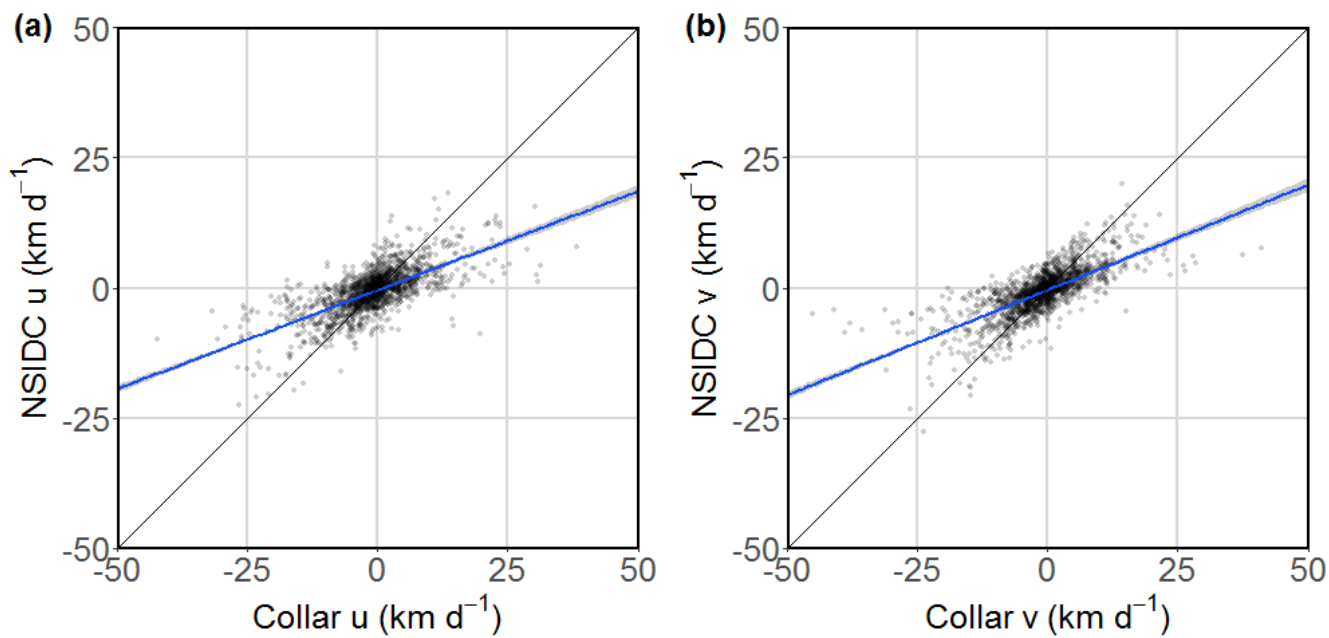
445 **Figure 5.** Accuracy of NSIDC drift speed represented by (a) histogram and density plot of the absolute accuracy ($Speed_{NSIDC} - Speed_{collar}$) and (b) GLM_{PQL} of relative accuracy ($Speed_{NSIDC}/Speed_{collar}$) as a function log-transformed collar speed (presented on log-log scale; blue line is the GLM_{PQL} prediction of the mean with shaded 95 % CI). In both A and B, data points are separated into three groups (red, purple, and blue) based on collar speed to convey speed-specific variability in accuracy. Black lines represent 1:1 unanimity between NSIDC and collar drift speeds.



450 **Figure 6.** Accuracy of NSIDC drift direction represented by (a) circular histogram and density plot of the absolute accuracy ($Direction_{NSIDC} - Direction_{collar}$) and (b) GLMM_{PQL} of relative accuracy ($\tan(|Direction_{NSIDC} - Direction_{collar}|/2)$) as a function of log-transformed collar speed (presented on a log-log scale, with a zero value representing 1:1 unanimity); blue line in represents the GLMM_{PQL} prediction of the mean with the shaded area representing the 95 % CI. Data points are separated into three groups (red, purple, and blue) based on collar speed to convey speed-specific variability in accuracy.



455 **Figure 7.** Difference in between collar drift and NSIDC drift v and the u components. Curves represent density of differences and the red dot represents the mean difference of u and v components.



460 **Figure 8.** GLMM_{PQL} (family: Gaussian) regression of the u (a) and v (b) components of NSIDC drift vector versus collar drift. Black lines represent a 1:1 relationship between NSIDC and collar drift components; the blue lines represent the lines of best fit with the shaded areas representing 95 % CI of the mean.